Cell-cycle regulator Whi5 shapes proliferative heterogeneity in clonal populations

Irene Delgado-Román, María José García-Marcelo, Lidia Delgado-Ramos, Sebastián Chávez and Mari Cruz Muñoz-Centeno.

Instituto de Biomedicina de Sevilla, Universidad de Sevilla-CSIC-Hospital Universitario V. del Rocío, and Departamento de Genética, Facultad de Biología, Universidad de Sevilla, Seville, E-41012, Spain.

* Mari Cruz Muñoz-Centeno.

Email: mcmunoz@us.es

Author Contributions: I.D.R. performed most experiments, analyzed data, contributed to discussions and prepared the figures; M.J.G.M. performed specific experiments at the final stages and contributed to figures; L.D.R. performed research at the initial stages; M.C.M.C. and S.C. designed research and discussed results; M.C.M.C. wrote the manuscript.

Competing Interest Statement: The authors declare no conflict of interest.

Keywords: Proliferative heterogeneity, replicative age, cell microencapsulation, Whi5.

Abstract

Clonal populations exhibit phenotypic variation in spite of being composed of genetically identical cells under equal environmental conditions. Proliferation rate also shows this heterogeneity, but the mechanisms underlying are still poorly understood. Cell cycle regulation controls proliferative capacity and previous transcriptomic studies revealed that budding yeast microcolonies with low proliferation rates display high levels of the G1-S transition inhibitor Whi5. In this work, we combined single cell microencapsulation with confocal microscopy to study heterogeneity in clonal cultures. We found that most slow-growing microcolonies are founded by young mother cells with a very short number of cell division cycles. This reduction in proliferation capacity is related to the expression levels of Whi5, which increases with the number of mother cell replication rounds since early stages. Our results establish that the proliferative structure of a cell population is cumulatively shaped in every mitotic cycle from the very first division, when a mother cell has the opportunity to increase Whi5 expression levels and to develop a slow proliferating lineage.

Introduction

Heterogeneity can be defined as the presence of different features within a population [1–3]. Differences among cells within the same clonal culture can arise by mutations accumulated during population growth. In addition to this genetic heterogeneity, which is relatively well understood[4–9], there is also phenotypical heterogeneity, observed in isogenic populations, that does not depend on mutations or environmental changes. In this latter case, heterogeneity can be present in any aspect of cell phenotype, like shape, size or differential expression of particular genes [10–13]. Phenotypical heterogeneity can also deal with the capacity of isogenic cells to divide and proliferate.

Proliferative heterogeneity explains variations in growth rate within a cell culture, as it has been repeatedly observed in the budding yeast *Saccharomyces cerevisiae* [12,14]. We have previously described that encapsulation of single cells from a yeast clonal population in alginate microspheres produce a wide range of microcolony sizes, due to differences in their proliferation rates [15].

The first events that lead to these different proliferation patterns may come from small stochastic fluctuations in the expression profile, commonly designed as “noise”, that produces differences in proliferation [10,16] . If this fluctuation affects critical genes, as it has been described for the histone

acetyltransferase *SIR2*, epigenetic changes can lead to stable expression patterns that provoke alteration in proliferation rates [17–19].

Epigenetic changes are frequently connected to aging and senescence. It has been demonstrated that very old *S. cerevisiae* mother cells, after more than 20 replication cycles, progressively lose proliferative capacity until they reach senescence[20–22]. The aging process of mother cells is characterized by accumulation of oxidative reactive species (ROS), increased DNA damage, loss of DNA repair capacity and failure to activate cell cycle checkpoints[23–25]. Very old cells are also deficient in the mechanism of asymmetric partitioning between mother and daughter cells, which prevents extrachromosomal rDNA circles and other aging factors to reach the latter [26–29]. The combination of these aging phenotypes contributes to increased generation time, provoking proliferative heterogeneity [30–34] and ultimately lead to cell senescence and death [35,36]. Although the whole *S. cerevisiae* lifespan has been studied, significant conclusions have been achieved from mother cells after a high number of divisions. However, the consequences on proliferation of the very first mitotic rounds (from 1 to 5) it has not yet been addressed. This very early effect is crucial to deeply understand the proliferative heterogeneity in clonal exponential cultures, where very most cells are new-born and their recent descendants, whereas old mother cells are very underrepresented [37].

In previous works, we performed transcriptomic analyses of yeast microcolonies according to their size, which revealed differential gene expression profiles between fast- and slow-growing clonal subpopulations [15]. The most differentially overexpressed gene in small microcolonies turned out to be the G1-S transition regulator Whi5[17], which represses expression of G1 cyclins by inhibiting the transcription factors SBF and MBF[38–40], in a similar manner to how Retinoblastoma protein controls G1-S transition in mammalian cells[41,42]. It has been proposed that Whi5 levels acquired by daughter cells during budding is essential for size-dependent entry into G1 [43]. It has been also described that Whi5 accumulates in very old cells, causing cell cycle delays and genomic instability that ultimately result in senescence and cell death[44].

These results led us to explore whether growth rates of microcolonies might be influenced by founder cell age, and whether variation of Whi5 levels might contribute to proliferation heterogeneity of populations that are genetically identical but intrinsically diverse in age. To answer these questions, we combined single cell microencapsulation with confocal microscopy and found that slow-growing microcolonies are frequently founded by mother cells, instead of the most abundant new-born cells. Surprisingly, we also found that these founders of slow-growing microcolonies were not aged cells, but young mothers with less than five divisions cycles. We also found that this

reduction in the proliferation capacity of microcolonies founded by young mother cells is related to the expression levels of Whi5, which increases with mother cell age since the very first division. Our results establish that the proliferative structure of a cell population is shaped in every mitotic cycle, when a mother cell has the chance to increase Whi5 expression levels and develop a slow proliferating lineage.

Results

A new method to analyze the replicative age of cells within a yeast microcolony

We have already shown that encapsulated microcolonies can be handled like particles suspended in a fluid, allowing, for example, their analysis in a large particle flow cytometer[14]. We conceived that it would also enable to perform the 3D analysis of individual microcolonies by confocal microscopy. We wondered whether such 3D analysis would help us to explain why some cells generate microcolonies at a lower proliferation rate than others.

We first established the criteria to microscopically detect those microcolonies with the most reduced proliferative rate. As described in Supplementary figure 1A, we considered “small” microcolonies (S) those with a diameter lower than 25 µm after encapsulation and 13 hours of incubation in optimal conditions. We considered “big” (B) microcolonies those larger than 50 µm in diameter, and “medium” (M) those in between 25 and 50 µm in diameter. As it is shown in Supplementary figure 1B, less than 30% of the microcolonies generated corresponded to the small category, presenting low proliferative capacity; more than 50% showed the size criteria to be defined as medium, and less than 20% were big ones.

In order to get insight on the genealogical structure of the microcolonies is important to know the replicative age of their cells. The number of bud scars is a perfect marker of replicative age. We proved that bud scars of encapsulated cells can be optimally detected after calcofluor staining, without affecting microcolony integrity as is shown in Supplementary figure 2.

After calcofluor staining, small microcolonies were analyzed under a confocal microscope. For each single small microcolony, we counted the total number of cells, as well as the number of bud scars present in each cell going through all Z axis images. We collected this data for more than 100 small microcolonies and analyzed the distribution of bud scars per cell in order to infer genealogic patterns (supplementary table S1 and supplementary data: all images used in this study can be found at http://www.ebi.ac.uk/biostudies/ with the accession number S-BSST1071). As a quality control, we calculated the total number of bud scars (n) and checked whether it was compatible

with the total number of cells counted (N). The number of scars should be always higher than the number of cells minus two (n > N-2). All microcolonies that did not fulfill this condition, likely founded by aggregated cells, were discarded.

In most cases, the distribution of scar number was consistent with the classical exponential growth. In this case unbudded newborn cells (no scar) were the most frequent category, but never above 50%. This type of microcolonies also contained decreasing proportions of cells with one bud or more. The cell with the highest number of buds was identified as the likely founder of the colony. We called “isotropic” to this pattern of growth. The confocal analysis of a representative example of an isotropic small microcolony is presented in Figure 1A. In this example, the small microcolony is composed by 8 cells, indicating that after microencapsulation of a single cell, 7 divisions took place. The cell exhibiting 5 bud scars was identified as the founder. Four cells were newborns with no bud scars, and the other 3 cells showed an intermediate number of bud scars, indicating that they had divided during the development of the microcolony. The representation of a potential sequence of division events that explain the distribution of scars is shown in Figure 1B. Under this isotropic pattern, although the proliferation rate was low and only produced 8 cells in 13 h, no particular cell in the microcolony showed a stronger restriction to divide.

A second growth pattern was also detected in some small microcolonies. In this case the founder cell underwent division several times, but its daughter cells did not, or showed severe restrictions to do it. We called “anisotropic” to this pattern of growth. The confocal analysis of a representative example of an anisotropic small microcolony is presented in Figure 1C. In this example the small microcolony presented 5 cells, indicating that 4 divisions took place after encapsulation of a single cell. The cell exhibiting 4 bud scars was identified as the founder. Three cells were newborns with no bud scars, and there was only one single-budded additional cell. This distribution of bud scars per cell, indicates that all but one of these divisions were undergone by the founder. The representation of a potential sequence of division events that explain the anisotropic development of this microcolony is shown in Figure 1D.

Once we defined these two growth patterns, we quantified how many of the small microcolonies analyzed corresponded to each of them. We observed that most of them (83 out of 93) presented an isotropic growth pattern, while only 10 exhibited the anisotropic one (Table 1, Supplementary Table 1 and Supplementary images at http://www.ebi.ac.uk/biostudies/).

Small microcolonies are more frequently founded by non-newborn cells

To address whether replicative age contributes to the proliferation heterogeneity shown by clonal cells, we decided to identify the founder cell in each small microcolony and to estimate its replicative age at the time of foundation. As mentioned above, by counting the number of bud scars in all cells that compose a microcolony, it is possible to identify the founder cell. In order to estimate its replicative age at the encapsulation moment (A), we reasoned that the replicative age of the founder cell at the time of encapsulation must fit with the difference between the total number of bud scars in the microcolony (n) and the total number of cells (N) plus one. ($A = n - N + 1$) (see Materials and Methods).

In the example of Figure 1A-B, the 8 cells of the microcolony exhibited 11 bud scars in total, which indicated that the founder cell had divided already three times before founding the microcolony. In the second example (Figure 1C-D) the 5 cells showed 4 bud scars, which indicated that the founder cell was a newborn. Using this simple calculation, we were able to estimate the replicative age of the founder cells of the 93 small microcolonies analyzed (Supplementary Table 1). According to our analysis, most small microcolonies were founded by non-newborn cells. This result was observed in both isotropic (more than a half) and anisotropic (nine out of ten) microcolonies (Table 1).

To really understand the relevance of this proportion of non-newborn cells as small microcolonies founders, we compared the age distribution of the founder cells (at the time of microencapsulation) to that of cells in an exponential liquid culture. As previously described [45], most of the cells in the exponential culture were newborns (about 64%). Decreasing proportions of cells containing from 1 to 3 and more bud scars were also detected (Figure 2A in grey). Since we used exponential liquid cultures for cell microencapsulation, we would expect the same age distribution in the founder cells of small microcolonies. In contrast, the age distribution of small microcolonies founder cells (in red) was significantly different ($p < 3.6 \times 10^{-5}$) (Figure 2A): much fewer newborn founders than in the liquid culture, and higher frequency of founders that had undergone some divisions before encapsulation than expected (Figure 2A and Supplementary figure 3).

We also studied more in detail the size of these small microcolonies in relationship with the age of the founder cell. We found that most small microcolonies founded by newborns consisted of more than 16 cells, whereas most of those founded by mothers with three or more previous divisions exhibited less than 16 cells (Figure 2B). Small microcolonies founded by young mothers (one or two previous divisions) showed an intermediate size distribution (Figure 2B). These results indicate that a slight increase in the founder cell age is concomitant with a decrease in the proliferation rate of the microcolony.

The fact that microcolonies founded by very young mother cells exhibited a significant higher tendency to be small argues for a negative influence of replicative age on cell proliferation since the earliest lifespan stages. In order to confirm this first conclusion of our study, we took advantage of the "Mother Enrichment Program" (MEP), an inducible genetic system, regulated by the presence of estradiol, which restricts the replicative capacity of daughter cells while allowing mother cells to achieve a normal replicative lifespan (Supplementary figure 4A) [46]. In the absence of estradiol, mother and daughter cells can divide normally. However, in the presence of estradiol, daughter cells become unviable and the population enriches in mother cells of increasing age.

We hypothesized that a slightly aged population, not dominated by newborns but by young mother cells that had already undergone one or two divisions, would increase the proportion of slow proliferating microcolonies after encapsulation. We first optimized the estradiol treatment required by the MEP strain DNY51 to undergo the very mild aging effect that we needed. We found that 3 h of incubation with estradiol was optimal to set a population with half of the newborns shown by the control culture and significant enrichment in mother cells with one or two bud scars (Supplementary figure 4B). While in the untreated population more than 60% of the cells were newborn, in the estradiol-treated culture 60% of the cells had budded once at least (Supplementary figure 4B).

These two cell populations were encapsulated and incubated for additional 13 hours in the absence of estradiol, to allow microcolonies formation without additional selection against daughter cells. Then, microcolonies were classified according to their size, as described in Supplementary figure 1A, and compared (Figure 2C). We found that the proportion of small microcolonies increased in the particles seeded with estradiol-treated cells as compared to the control samples, being the predominant microcolony category in this condition. The overall distribution of microcolony size was significantly altered by the short number of division cycles previously undergone by the founder cells (Square Chi test $p < 0{,}001$). This result strengthened the link between replicative age and proliferation rate, already in the very first stages of a mother cell lifespan, indicating that, once a daughter cell divides, there is a significant probability of its descending lineage to stably slow down its proliferation rate across generations.

Whi5 levels set proliferation rate during microcolony development

As mentioned in the Introduction, in our transcriptomic analysis we had found that slow- and fast-proliferating microcolonies exhibited differential transcriptomic signatures. Specifically, *WHI5* was the most overexpressed gene in small microcolonies[14]. In budding yeast, Whi5 is a G1/S transition inhibitor [42] that contributes to both, the determination of critical cell size at START and cell fate [47–

[50]. We decided to confirm that this correlation between Whi5 high levels and slow-proliferating (small) microcolonies was causative, in the sense that Whi5 levels determined slow proliferation and not vice versa. To do that, we used the *S. cerevisiae* KSY098 strain[51], where *WHI5* gene expression is under the regulation of chimeric regulator containing an estrogen-binding domain and responds to estradiol in a dose-dependent manner[52] (Figure 3A).

First, as shown in Figure 3B, we compared the microcolonies produced by encapsulated KSY098 cells, cultured in the absence of estradiol (referred as control in the B panel) and, therefore, expressing undetectable levels of Whi5 (Figure 3A), to those produced by isogenic W303 cells, which express *WHI5* from its own promoter. Lack of Whi5 expression produced a significant shift of the microcolony distribution towards the big category at the expense of medium and small ones (Figure 3B). This result confirmed that Whi5 plays a role in the proliferation heterogeneity detected in our microcolony assay and its expression is detrimental for the fast-growing subpopulation.

This result prompted us to hypothesize that, on the contrary, higher levels of Whi5 should favor slow-proliferating microcolonies. To test this hypothesis, we encapsulated exponentially growing KSY098 cells, in the absence of estradiol (not expressing *WHI5*). Single-cell seeded particles were then incubated without estradiol or in the presence of estradiol concentrations ranging between 2 and 10 nM (see Supplementary figure 5 for a synopsis of the experiment). Interestingly, cells incubated after encapsulation with 4nM estradiol showed a significant change in the microcolony distribution towards the small category, at the expense of the big one (Figure 3C). Higher concentrations of estradiol, which produced stronger expression of Whi5 (Figure 3A), also caused higher frequencies of small microcolonies (Figure 3C).

The proportion of cells expressing high Whi5 levels increases after the first mitotic cycles

The results described above confirmed that small microcolonies associates with high Whi5 levels. We have also showed in this work that such small or slow-proliferating microcolonies were frequently founded by cells that had undergone more than one previous division cycle. We wondered whether these two phenomena were linked, in a way that Whi5 levels increase with the number of mitotic cycles.

To test this hypothesis, we analyzed cells expressing a Whi5-GFP fusion as the sole source of Whi5, and controlled by the endogenous *WHI5* promoter. Exponentially growing Whi5-GFP cells were sorted and collected according to their GFP signal, as described in detail in Material and Methods (see Supplementary figure 6 A and B for a synopsis of the experiment). We collected three different type of samples: i) cells with the highest Whi5-GFP expression (represented in

green); ii) cells with the lowest Whi5-GFP expression (represented in purple); iii) a random sample of the whole population as a control (represented in blue) (Figure 4A). After that, each sample was stained with calcofluor and analyzed under the microscope to obtain the replicative age distribution of cells. We found the expected distribution of bud scar counts in the control sample, the random sample of the whole population (compare blue bars in Figure 4A). In contrast, when we analyze the distribution of bud scars in the sample with low Whi5-GFP levels a significant enrichment in newborn cells was observed (purple bars in Figure 4A). Moreover, the replicative age distribution of cells sorted for high Whi5-GFP levels presented a very clear reduction in newborn cells and an enrichment in cells with two or more division cycles (green bars in Figure 4A).

To analyze more in detail these results, in Figure 4B we represent, for each replicative age category, the ratio of number of cells with higher Whi5 levels (green) versus the total in this category. Considered altogether, these results show that mother cells can increase Whi5 expression as they undergo division cycles since the earliest stages of their lifespans.

Young mother cells exhibit longer S-G2-M phases and overexpress Whi5 before cytokinesis

The correlation observed between decreased proliferation rate and higher Whi5 levels in young mother cells prompted us to investigate how this increase in Whi5 is achieved. It is well-established that *WHI5* mRNA accumulates during the S-G2-M phases of the cell cycle [53,54]. Thus, we decided to investigate if the duration of these cell cycle phases was altered when a newborn cell performs the first division rounds.

In order to study cell cycle progression in young mother cells, we decided to perform a G1 synchronization and release assay. To do that, we first performed the biotin-streptavidin purification assay already described (see Materials and Methods) and enriched cultures in very young mother. Differences in cell populations according to their replicative age after enrichment are displayed in supplementary Figure S7. We observed that after 6 hours of treatment, the culture became severely depleted of newborns and dominated by mother cells with 2 to 5 divisions.

The culture enriched in young mother cells and a control one, where newborns were predominant, were then synchronized in G1 with alpha-factor and allowed to progress into a new cell cycle. Samples were collected every 5 minutes and analysed by flow cytometry. As we can observe in Figure 5A and B, young mother-enriched cultures (pink) progressed earlier into S phase compared to the new born enriched culture (blue): while the young mother-enriched culture came out of G1 al 15-20 minutes, the exponential culture with a high proportion of new born cells, spent at least 5 more minutes to start entering S phase. This delay was consistent in five independent experiment

and statistically significant (Figure 5A). Interestingly, despite the earlier entry into S phase of young mother cells, both cultures exited G2/M phase at the same time, indicating that S-G2-M segment of the cell cycle was longer in young mothers compared to new-born cells (Figure 5A-B).

As mentioned above, *WHI5* expression peaks in S and G2/M phases. We hypothesized that the relative longer S-G2-M duration in young mothers could lead to higher Whi5 concentration by elongating the time at which *WHI5* is being expressed. In order to test this, we decided to carry out a qPCR analysis of *WHI5* mRNA levels after alpha-factor synchronization and release. Thus, we performed the same biotin-streptavidin purification and alfa factor synchronization as described in the previous paragraph but, this time, samples were collected at specific time-points. To choose these time-points, samples from the previous experiment were also analysed under the fluorescence microscope, in order to determine the cell cycle step of each of these cells more in detail by cell morphology and nuclei visualization (Figure 5C right panel, and supplementary Table S2). We then chose the time-points with more enrichment in every cell cycle phase category from four different replicas and we analysed them by RP-qPCR. As it is shown in Figure 5C, *WHI5* mRNA levels decreased from S to telophase in control cells but remained high in young mothers, resulting in a highly significant accumulation in this latter category. This result indicates that young mother cells are prone to accumulate Whi5 in the S-G2-M segment, before cytokinesis and the initiation of a new G1 phase of the cell cycle.

Discussion

Proliferative heterogeneity is coupled to mitotic division since very early stages

Heterogeneity in clonal populations can take many shapes, including very different proliferation rates[30]. We have focused on proliferative heterogeneity as we previously described that microencapsulated isogenic single cells produced microcolonies with a wide rank of sizes[14]. This heterogeneity in size reflects the number of cells that form the microcolony and, therefore, to a difference in the number of divisions undergone during its formation.

To understand proliferative heterogeneity, studies cannot be performed in culture populations but analyzing individual cells and colonies. We have developed a direct and powerful methodology to

analyze the generation of individual microcolonies from a single founder cell, by combining cell microencapsulation and confocal microscopy. Using this new experimental strategy, we have uncovered two different types of growth patterns associated to low proliferation rates. In the most frequent one (83 out of 93 small microcolonies analyzed), that we called “isotropic” growth, all cells proliferate at low rate and no particular cell in the microcolony showed a stronger restriction to divide. The second small microcolony generation pattern, that we called “anisotropic” growth, is less frequent (10 out of 93 small microcolonies analyzed) and involves that, while the founder cell undergoes division several times, its daughter cells do not, or show severe restrictions to do it. Anisotropic growth might be caused by the mild stress that founder cells may undergo during microencapsulation, as described for low-metal environment[55]. The fact that only 10 out of 93 small microcolonies analyzed follow this growth pattern, whereas 83 out of 93 followed the isotropic one, suggests that the conclusions reached in this study are not restricted to stressed cell sub-populations.

Our analyses also provide relevant information on the age of founder cells at the moment of encapsulation, that is, when slow-growing microcolonies were initiated. According to our analyses, most slow-proliferating microcolonies were founded by non-newborn cells after performing less than 5 divisions, both in isotropic and anisotropic types. While the liquid cultures used for encapsulation presented the well-known distribution of cell ages of exponentially growing populations [56–58], characterized by a majority of newborn cells without bud scars (64%) followed by progressively reducing subpopulations of cells with 1, 2, 3 and more bud scars (Figure 2A), slow-proliferating microcolonies founder cells did not fit this proportion. In fact, they were enriched in cells that had performed one or more divisions before encapsulation (Figure 2A). Moreover, the smaller the microcolony, the higher the number of division cycles previously undergone by the founder cells (Figure 2B). Finally, using the MEP system to enrich in non-newborn founder cells (1 or 2 divisions) we got a significant increase in slow-proliferating microcolonies (Figure 2C). We conclude that once a newborn cell divides, there is a significant probability of its descending lineage to stably slow down its proliferation rate across generations. In other words: the restriction in proliferation capacity can be established in any stage of the mother cell lifespan, even during its first division cycle.

It is important to emphasize that the impact in proliferation rate that we describe takes place at the very early stages of the replicative lifespan, since this connection has been so far studied from the perspective of the last divisions that a mother cell undergoes before death, after more than 10 replicative cycles [36,59,60]. Secondly, the impact on proliferation rate from the very first divisions gives better understanding on the proliferative heterogeneity observed in exponential cultures, where the

proportion of cells with more than 10 divisions is quite insignificant. In fact, restricted proliferation of young mother cells produces a much greater impact on population fitness than does functional deterioration at later ages and may play a substantial role in adaptations to changing environments[30].

Whi5 levels link proliferative heterogeneity to very early stages of the replicative lifespan

Cell cycle progression requires complex regulatory networks in eukaryotic cells to ensure functional success[61]. Timing of Start at late G1 is regulated by the antagonistic interplay between the Cln3 G1 cyclin and the Whi5 inhibitor [38]. Increased synthesis of Cln3 and dilution of Whi5 levels due to cell size increase has been proposed to control Start timing and cell size-dependent proliferation [50] (Schmoller et al., 2015b). As cell size increases, Whi5 protein would be progressively diluted and, once it has reached a certain threshold concentration, which should correspond to an optimal division size, cells commit to division [48]. In this work we found a strong connection between Whi5 concentration and proliferation heterogeneity. By modulating its expression, we showed a direct correlation between Whi5 levels and the proportion of slow-proliferating microcolonies (Figure 3A-C). Furthermore, the sorting results shown in Figure 4 demonstrate that higher Whi5 levels associates start to non-newborn cells that have undergone a short number of replicative cycles. These results confirmed our previously published finding that smallest microcolonies, mostly founded by non-newborn cells, overexpressed Whi5[14].

It has been previously described that Whi5 accumulates in very old aged cells, causing cell cycle delays and genomic instability that ultimately result in cell death[44]. However, this description was based on mother cells after more than 10 division cycles, closed to the end of its life span. Here we present results showing that young mother cells, after only 1 to 5 divisions, displayed longer S-G2-M phases than newborn cells (Figure 5A-B) and accumulated significant higher levels of Whi5 (Figure 4) due to increased expression before cytokinesis (Figure 5C). Our results demonstrate that accumulation of Whi5 can happen at any division of a mother cell, since very early stages, and allow us proposing Whi5 as the key regulator of proliferation heterogeneity across generations.

Increase of Whi5 might be due to stochastic noise in its expression, but might also be linked to its time of expression during the cell cycle, which seems to be maximal in S and G2/M phases [62]. Any delay in progression through S or G2/M might provoke increased Whi5 levels. Our results show that young mother cells tend to increase the length of this expression window and to accumulate higher levels of *WHI5* mRNA before cytokinesis (Figure 5A-C).

It has been recently shown that Whi5 not only regulates G1/S transition but also progression through S/G2/M [63]. Accordingly, alteration of the mitotic cycle in S/G2/M, due for instance to

activation of checkpoint mechanisms, might provoke increased Whi5 levels, which in turn would induce subsequent cell-cycle alterations, enabling a self-regulatory loop that would propagate throughout the cell linage. Such activation of checkpoints has been described to play a role in mitotic catastrophe during late aging [64]. Our work suggest that it may be a more common phenomenon, potentially being triggered in any stage of replicative life span, and explaining the high proliferative heterogeneity of cell populations.

The combination of all our results is compatible with a model (supplementary Figure S8) in which a cell with optimal proliferation capacity can undergo increased Whi5 expression at any division cycle, since the very first. This increase in Whi5 levels would negatively condition the proliferation rate of its progeny, favoring extensive growth heterogeneity of the whole population. We have previously shown that reduced proliferation rate is linked to other phenotypic features like energy metabolism, since small microcolonies respirate within the same cultures where fast-growing cells are fermenting[14] . Slow growth is also associated to altered mRNA turnover and a different global pattern of gene expression [14]. In this sense, Whi5-dependent proliferation restrictions would not be just a terminal phenomenon linked to aging and senescence, but a developmental process that allows cell differentiation, in terms of growth rate within the population, increasing its phenotypic diversity.

Materials and Methods

Strains

See supplementary table 3 for a list of all strains used in this work.

Microencapsulation

Microencapsulation conditions were set to obtain single cell clonal cultures inside every capsule. First, cells were cultured to a O.D. $_{600nm}$ of approximately 0.5 to ensure that it was at exponential growth phase. Microencapsulation of individual yeast cells in alginate microparticles was performed using a Cellena microencapsulator (Ingeniatrics) following the protocol already published [14,15]. After microencapsulation, capsules were collected and cultured together in YPD for 13 hours at 30ºC continuous stirring.

Mother cell enrichment by selection against newborns

DNY51 strain was used for mother cell enrichment as described [46]. A graphical explanation of the Mother Enrichment Programm developed by Lindstrom and Gottschling is shown in supplementary Figure S4A. DNY51 cells were grown at normal culture conditions to exponential phase, they were then collected and inoculated in 10ml of YPD (previously preheated at 30ºC) with 1μM estradiol. They were cultured at 30ºC for 3 hours. The estradiol was then washed out, and cells were resuspended in YPD to finally add them to the microencapsulation mixture. After microencapsulation, capsules were collected and cultured in YPD (without estradiol) for 13 hours at 30 ºC.

Modulation of Whi5 expression

KSY098-1 strain, kindly provided by Kurt Schmoller, allowed us to modulate *WHI5* expression, which in this strain is under the transcriptional control of an estrogen receptor derivative [51]. A KSY089-1 culture was first growth to exponential phase ($O.D._{600nm}$ of 0.5) and then microencapsulated following the usual protocol. After that, microcapsules were collected and then inoculated in flasks with YPD and estradiol at different concentrations (0, 2, 4, 6, 8 and 10 nM). The wildtype W303 control was separately encapsulated the same day. Finally, these and the W303 wildtype strain were cultured for 9,5 hours at 30º C.

Light microscopy and microcolony size analysis

Microcolony size analyses were performed using a Leica DM750 optical microscope. Microcolonies were classified according to their size in small, medium and big microcolonies. As capsule diameter is stable (approximately 100μm), big microcolonies were considered those that surpass the radio of the capsule, medium microcolonies were those whose size range between half the radio and the radio, and those that were smaller than half the radio were considered small microcolonies (Supplementary Figure 1A).

Calcofluor staining

For replicative age analysis bud scar staining was performed. First, cells were collected at exponential growth phase, fixated with 70% Ethanol and stored at 4ºC for at least 2 hours. After that, cells were washed with PBS 1X and resuspended in a solution of PBS and calcofluor (Fluorescent Brightener 28, Sigma Aldrich) at a final concentration of 0.1 mg/ml. They were incubated for 5 to 10 minutes in dark conditions at room temperature and then washed again with PBS. Cells were finally resuspended in 100μl of PBS.

Microcolonies were also stained with calcofluor for small microcolonies founder cell identification. First, fixated microcolonies (YPD and Ethanol 70% 1:1) were filtrated and collected. They were

washed with a TrisHCl-CaCl 2:1 solution and inoculated in 0.5 ml of calcofluor at 0.1 mg/ml concentration for 5 min at room temperature. After that, microcapsules were filtrated and washed again with TrisHCl-CaCl solution. Finally, they were collected and preserved in 0.5 ml of the same solution.

Fluorescent microscopy and bud scar counting

Replicative age of the population was calculated by manually counting the number bud scars per cell using a direct fluorescent microscope Olympus BX-61. Bud scars of calcofluor-stained cells were detectable using the DAPI filter.

Confocal microscopy and founder cells age analysis

Microcolonies stained with calcofluor were visualized in a A1R Confocal Nikon Microscope using the 60X oil objective and DAPI filter. Images of small microcolonies (n=187) were taken every 0.5 μM in Z-axis. Total number of cells and total number of bud scars were counted going through all Z axis images. Using the formula $number\ of\ budscars - number\ of\ cells + 1 = founder\ cell\ age$ the replicative age of the small microcolonies founder cells at initial time (right before founding the small microcolony) was estimated. The resulting number was corrected when incoherent: very high numbers usually meant that the small microcolony was founded by two aged cells. These cases were taken out of the analysis. On the other hand, negative numbers probably meant that the number of bud scars was underestimated. Going through the genealogy of the small microcolonies, taken into consideration the number of buds observed on each cell, these numbers were corrected according to the most probable scenario (being usually the case of a newborn founder).

Whi5-GFP cell sorting

Whi5-GFP strain was cultured to exponential growth in minimum complete media. Then, cells were collected at of OD_{600nm} of 0.5 and sorted in a BD FACSJazz™ cell sorter according to the GFP intensity detected. Cells with high Whi5 expression were considered the 5% with the highest GFP expression. After sorting, each sample was stained with calcofluor and analyzed for bud scar counting.

Mother enrichment in synchronized cultures by biotin/streptavidin purification

Cells were collected at an $O.D._{600nm}$ of 0.4. They were then centrifuged at 4,000 rpm for 4 minutes, washed twice with 1ml PBS (2 minutes at 6,000rpm) and incubated with 10 mg of biotin for 30 minutes. Half of the culture was collected as control cells (non-enriched in mother cells) and was incubated in YPAD for 30 minutes in agitation at 30ºC. The rest of the culture was incubated for 6

hours in the same conditions. After each incubation, cells were treated with 1µg/ml of alfa-factor for 2 hours (or until the shmoo structure is visible under the microscope). After this, we performed a streptavidin extraction (New England Biolabs, 150 µl per sample) for 30 minutes at room temperature using streptavidin-linked magnetic beads. The supernatant was discarded and the cells attracted by the magnet were washed several times. After this step, cells were washed and inoculated into fresh YPAD media (previously heated at 30ºC) with pronase at 50µg/ml. Samples were collected every 5 minutes for the following 90 minutes and fixated in 500 µl of 70% ethanol.
In these experiments, we ensured that mother cell enriched cultures had the mean replicative age of our interest by staining with calcofluor and counting the number of budscars.

Propidium iodide staining and flow cytometry

Fixed cells were washed twice with 1ml of sodium citrate 50mM and then treated with 500µl of sodium citrate with RNAase overnight. After this, 500 µl of a solution of propidium iodide (PI)(4µg/ml) and sodium citrate 50 nM was added to every sample. Cells were incubated for 30 min at room temperature and dark conditions.
For flow cytometry, samples were sonicated during 3 cycles of 1 min (30 seconds of sonication for every cycle). After this, cell cycle analysis was performed using a BD FACSCanto™ Clinical Flow Cytometry System. Cells were classified according to their PI content, which correlates with DNA content. This allows sorting cells into G1 cells (1 content of DNA) and G2/M (2 contents of DNA).

***WHI5* RTqPCR analysis in synchronized young mother cells**

In order to determine Whi5 mRNA levels for every cell cycle phase, samples of synchronized cultures were collected and then analyzed by RTqPCR. First, cultures were collected at exponential growth and enriched in mother cells using the same protocol described above. After alfa-factor treatment, cells were enriched in mother cells (early aged cells) through streptavidin extraction and then inoculated into YPAD and pronase. 15 ml samples were collected at the indicated times for every experiment and then washed and frozen in liquid nitrogen. For every timepoint, 20 ml samples were used for RT-qPCR and an additional sample was analyzed by flow cytometry and microscopy, in order to check the actual cell cycle phase.
Quantitation of *WHI5* mRNA levels by RT-qPCR was carried out using the following primers: 5' GGCTGCGCGTCGGTCTAC 3' and 5' TGCAGCTTGACTAACGCGTAAT 3'. It was performed in a LightCycler® 480 Instrument II thermocycler (Roche). For each reaction we used 4 µl of sample and 6 µl of a mixture with forward and reverse oligonucleotides and Sybr Green Premix.

Acknowledgments

We thank all the people of the IBiS Gene Expression lab for helpful discussion and all technicians from IBiS and CITIUS facilities. We deeply thank Kurt Schmoller and Michael Chang and Daniel Gottschling for KSY098-1 and DNY51 strains, respectively. We also thank our colleagues of IBiS and the Genetics Department of Universidad de Sevilla for their support.

Funding

This work has been supported by grants from the Ministerio de Ciencia e Innovación-Agencia Estatal de Investigación (BFU2016-77728-C3-1-P to M.C.M.C. and S.C. and PID2020-112853GB-C32 to M.C.M.C.), Andalusian Government and European Union funds (FEDER) (US-1256285 to M.C.M.C and BIO271 to S.C.).

References

1. Ackermann, M. A functional perspective on phenotypic heterogeneity in microorganisms. *Nature Reviews Microbiology* vol. 13 497–508 Preprint at https://doi.org/10.1038/nrmicro3491 (2015).

2. Ryall, B., Eydallin, G. & Ferenci, T. Culture History and Population Heterogeneity as Determinants of Bacterial Adaptation: the Adaptomics of a Single Environmental Transition. *Microbiology and Molecular Biology Reviews* **76**, 597–625 (2012).

3. Sánchez-Romero, M. A. & Casadesús, J. Contribution of phenotypic heterogeneity to adaptive antibiotic resistance. *Proc Natl Acad Sci U S A* **111**, 355–360 (2014).

4. Davis, K. M. & Isberg, R. R. Defining heterogeneity within bacterial populations via single cell approaches. *BioEssays* vol. 38 782–790 Preprint at https://doi.org/10.1002/bies.201500121 (2016).

5. Cota, I., Blanc-Potard, A. B. & Casadesús, J. STM2209-STM2208 (opvAB): A phase variation locus of salmonella enterica involved in control of O-antigen chain length. *PLoS One* **7**, (2012).

6. Sampaio, N. M. V. & Dunlop, M. J. Functional roles of microbial cell-to-cell heterogeneity and emerging technologies for analysis and control. *Current Opinion in Microbiology* vol. 57 87–94 Preprint at https://doi.org/10.1016/j.mib.2020.08.002 (2020).

7. Ghosh, D., Veeraraghavan, B., Elangovan, R. & Vivekanandan, P. Antibiotic resistance and epigenetics: More to it than meets the eye. *Antimicrob Agents Chemother* **64**, (2020).

8. Ziv, N., Siegal, M. L. & Gresham, D. Genetic and nongenetic determinants of cell growth variation assessed by high-throughput microscopy. *Mol Biol Evol* **30**, 2568–2578 (2013).

9. Olivenza, D. R. *et al.* A portable epigenetic switch for bistable gene expression in bacteria. *Sci Rep* **9**, (2019).

10. Newman, J. R. S. *et al.* Single-cell proteomic analysis of S. cerevisiae reveals the architecture of biological noise. *Nature* **441**, 840–846 (2006).

11. Martins, B. M. C. & Locke, J. C. W. Microbial individuality: how single-cell heterogeneity enables population level strategies. *Current Opinion in Microbiology* vol. 24 104–112 Preprint at https://doi.org/10.1016/j.mib.2015.01.003 (2015).

12. Levy, S. F., Ziv, N. & Siegal, M. L. Bet hedging in yeast by heterogeneous, age-correlated expression of a stress protectant. *PLoS Biol* **10**, (2012).

13. Lee, J. A. *et al.* Microbial phenotypic heterogeneity in response to a metabolic toxin: Continuous, dynamically shifting distribution of formaldehyde tolerance in Methylobacterium extorquens populations. *PLoS Genet* **15**, (2019).

14. García-Martínez, J. *et al.* The cellular growth rate controls overall mRNA turnover, and modulates either transcription or degradation rates of particular gene regulons. *Nucleic Acids Res* **44**, 3643–3658 (2016).

15. Delgado-Ramos, L. Microbial analysis by microencapsulation and its application to study proliferation heterogeneity. (Universidad de Sevilla, 2016).

16. Pelechano, V., Wei, W. & Steinmetz, L. M. Extensive transcriptional heterogeneity revealed by isoform profiling. *Nature* **497**, 127–131 (2013).

17. Kyu Kang, W., Hyeock Kim, Y., Ah Kang, H., Kwon, K.-S. & Kim, J.-Y. Sir2 phosphorylation through cAMP-PKA and CK2 signaling inhibits the lifespan extension activity of Sir2 in yeast. doi:10.7554/eLife.09709.001.

18. Song, J. *et al.* Essential Genetic Interactors of SIR2 Required for Spatial Sequestration and Asymmetrical Inheritance of Protein Aggregates. *PLoS Genet* **10**, (2014).

19. Smith, J. T., White, J. W., Dungrawala, H., Hua, H. & Schneider, B. L. Yeast lifespan variation correlates with cell growth and sir2 expression. *PLoS One* **13**, (2018).

20. Campisi, J. & D'Adda Di Fagagna, F. Cellular senescence: When bad things happen to good cells. *Nature Reviews Molecular Cell Biology* vol. 8 729–740 Preprint at https://doi.org/10.1038/nrm2233 (2007).

21. Mirisola, M. G. & Longo, V. D. Yeast Chronological Lifespan: Longevity Regulatory Genes and Mechanisms. *Cells* vol. 11 Preprint at https://doi.org/10.3390/cells11101714 (2022).

22. Michael Breitenbach, S. Michal Jazwinski & Peter Laun. *Aging Research in Yeast*. vol. 57 (Springer Dordrecht, 2012).

23. Fehrmann, S. *et al.* Aging yeast cells undergo a sharp entry into senescence unrelated to the loss of mitochondrial membrane potential. *Cell Rep* **5**, 1589–1599 (2013).

24. Yi, D. G., Hong, S. & Huh, W. K. Mitochondrial dysfunction reduces yeast replicative lifespan by elevating RAS-dependent ROS production by the ER-localized NADPH oxidase Yno1. *PLoS One* **13**, (2018).

25. Hao, N. *et al.* DNA damage checkpoint activation impairs chromatin homeostasis and promotes mitotic catastrophe during aging. (2019) doi:10.7554/eLife.50778.001.

26. Yang, J. *et al.* Systematic analysis of asymmetric partitioning of yeast proteome between mother and daughter cells reveals 'aging factors' and mechanism of lifespan asymmetry. *Proc Natl Acad Sci U S A* **112**, 11977–11982 (2015).

27. Sinclair, D. A. & Guarente, L. *Extrachromosomal RDNA Circles-A Cause of Aging in Yeast*. *Cell* vol. 91 (1997).

28. Morlot, S. *et al.* Excessive rDNA Transcription Drives the Disruption in Nuclear Homeostasis during Entry into Senescence in Budding Yeast. *Cell Rep* **28**, 408-422.e4 (2019).

29. Hull, R. M. & Houseley, J. The adaptive potential of circular DNA accumulation in ageing cells. *Current Genetics* vol. 66 889–894 Preprint at https://doi.org/10.1007/s00294-020-01069-9 (2020).

30. Knorre, D. A., Azbarova, A. V., Galkina, K. V., Feniouk, B. A. & Severin, F. F. Replicative aging as a source of cell heterogeneity in budding yeast. *Mechanisms of Ageing and Development* vol. 176 24–31 Preprint at https://doi.org/10.1016/j.mad.2018.09.001 (2018).

31. Xu, Z. & Teixeira, M. T. The many types of heterogeneity in replicative senescence. *Yeast* **36**, 637–648 (2019).

32. Kamei, Y., Tamada, Y., Nakayama, Y., Fukusaki, E. & Mukai, Y. Changes in transcription and metabolism during the early stage of replicative cellular senescence in budding yeast. *Journal of Biological Chemistry* **289**, 32081–32093 (2014).

33. Wang, Y., Lo, W. C. & Chou, C. S. A modeling study of budding yeast colony formation and its relationship to budding pattern and aging. *PLoS Comput Biol* **13**, (2017).

34. Vaiserman, A. M., Koliada, A. K. & Jirtle, R. L. Non-genomic transmission of longevity between generations: Potential mechanisms and evidence across species. *Epigenetics and Chromatin* vol. 10 Preprint at https://doi.org/10.1186/s13072-017-0145-1 (2017).

35. Frenk, S. & Houseley, J. Gene expression hallmarks of cellular ageing. *Biogerontology* **19**, 547–566 (2018).

36. Smith, J., Wright, J. & Schneider, B. L. A budding yeast's perspective on aging: The shape I'm in. *Exp Biol Med* **240**, 701–710 (2015).

37. Vanoni, M., Vai, M., Popolo, L. & Alberghina, L. *Structural Heterogeneity in Populations of the Budding Yeast Saccharomyces Cerevisiae*. *JOURNAL OF BACTERIOLOGY* (1983).

38. De Bruin, R. A. M., Mcdonald, W. H., Kalashnikova, T. I., Yates, J. & Wittenberg, C. *Cln3 Activates G1-Specific Transcription via Phosphorylation of the SBF Bound Repressor Whi5 Fall into the G1-Specific Gene Family (Cho et al They Govern the Events Associated with Cell Cycle Initiation, Including DNA Repli*. *Cell* vol. 117 (2004).

39. Wagner, M. V. *et al.* Whi5 regulation by site specific CDK-phosphorylation in Saccharomyces cerevisiae. *PLoS One* **4**, (2009).

40. Johnson, A. & Skotheim, J. M. Start and the restriction point. *Current Opinion in Cell Biology* vol. 25 717–723 Preprint at https://doi.org/10.1016/j.ceb.2013.07.010 (2013).

41. Cooper, K. Rb, whi it's not just for metazoans anymore. *Oncogene* vol. 25 5228–5232 Preprint at https://doi.org/10.1038/sj.onc.1209630 (2006).

42. Michael Costanzo *et al.* CDK Activity Antagonizes Whi5, an Inhibitor of G1/S Transcription in Yeast. *Cell* **117**, 899–913 (2004).

43. Schmoller, K. M., Turner, J. J., Kõivomägi, M. & Skotheim, J. M. Dilution of the cell cycle inhibitor Whi5 controls budding-yeast cell size. *Nature* **526**, 268–272 (2015).

44. Neurohr, G. E. *et al.* Deregulation of the G1/S-phase transition is the proximal cause of mortality in old yeast mother cells. *Genes Dev* **32**, 1075–1084 (2018).

45. Lee, S. S., Vizcarra, I. A., Huberts, D. H. E. W., Lee, L. P. & Heinemann, M. Whole lifespan microscopic observation of budding yeast aging through a microfluidic dissection platform. *Proc Natl Acad Sci U S A* **109**, 4916–4920 (2012).

46. Lindstrom, D. L. & Gottschling, D. E. The mother enrichment program: A genetic system for facile replicative life span analysis in Saccharomyces cerevisiae. *Genetics* **183**, 413–422 (2009).

47. Palumbo, P. *et al.* Whi5 phosphorylation embedded in the G 1 /S network dynamically controls critical cell size and cell fate. *Nat Commun* **7**, (2016).

48. Schmoller, K. M., Turner, J. J., Kõivomägi, M. & Skotheim, J. M. Dilution of the cell cycle inhibitor Whi5 controls budding-yeast cell size. *Nature* **526**, 268–272 (2015).

49. Schmoller, K. M. *et al.* Whi5 is diluted and protein synthesis does not dramatically increase in pre-Start G1. *Mol Biol Cell* **33**, lt1 (2022).

50. Litsios, A. *et al.* The timing of Start is determined primarily by increased synthesis of the Cln3 activator rather than dilution of the Whi5 inhibitor. *Mol Biol Cell* **33**, rp2 (2022).

51. Kukhtevich, I. V., Lohrberg, N., Padovani, F., Schneider, R. & Schmoller, K. M. Cell size sets the diameter of the budding yeast contractile ring. *Nat Commun* **11**, (2020).

52. Ottoz, D. S. M., Rudolf, F. & Stelling, J. Inducible, tightly regulated and growth condition-independent transcription factor in Saccharomyces cerevisiae. *Nucleic Acids Res* **42**, (2014).

53. Taberner, F. J., Quilis, I. & Igual, J. C. Spatial regulation of the start repressor Whi5. *Cell Cycle* **8**, 3013–3022 (2009).

54. Spellman, P. T. *et al. Comprehensive Identification of Cell Cycle-Regulated Genes of the Yeast Saccharomyces Cerevisiae by Microarray Hybridization □ D*. *Molecular Biology of the Cell* vol. 9 http://cellcycle-www.stanford.edu (1998).

55. Avraham, N., Soifer, I., Carmi, M. & Barkai, N. Increasing population growth by asymmetric segregation of a limiting resource during cell division. *Mol Syst Biol* **9**, (2013).

56. Lord, P. G. & Wheals, A. E. *Asymmetrical Division of Saccharomyces Cerevisiae*. *JOURNAL OF BACTERIOLOGY* vol. 142 (1980).

57. Lee, S. S., Vizcarra, I. A., Huberts, D. H. E. W., Lee, L. P. & Heinemann, M. Whole lifespan microscopic observation of budding yeast aging through a microfluidic dissection platform. *Proc Natl Acad Sci U S A* **109**, 4916–4920 (2012).

58. Keinan, E. *et al.* High-Reynolds Microfluidic Sorting of Large Yeast Populations. *Sci Rep* **8**, (2018).

59. S. Michal Jazwinski. Molecular mechanisms of yeast longevity. *Trends Microbiol* **7**, 247–252 (1999).

60. Egilmez, N. K. & Jazwinski, S. M. *Evidence for the Involvement of a Cytoplasmic Factor in the Aging of the Yeast Saccharomyces Cerevisiae*. *JOURNAL OF BACTERIOLOGY* vol. 171 (1989).

61. Delgado-Román, I. & Muñoz-Centeno, M. C. Coupling Between Cell Cycle Progression and the Nuclear RNA Polymerases System. *Frontiers in Molecular Biosciences* vol. 8 Preprint at https://doi.org/10.3389/fmolb.2021.691636 (2021).

62. Granovskaia, M. V. *et al.* High-resolution transcription atlas of the mitotic cell cycle in budding yeast. *Genome Biol* **11**, (2010).

63. Xiao, J., Turner, J. J., Kõivomägi, M. & Skotheim, J. M. Whi5 hypo- and hyper-phosphorylation dynamics control cell cycle entry and progression. *bioRxiv* (2023) doi:10.1101/2023.11.02.565392.

64. Crane, M. M. *et al.* Rb analog Whi5 regulates G1 to S transition and cell size but not replicative lifespan in budding yeast. *Transl Med Aging* **3**, 104–108 (2019).

Figures and Tables

A

Calcofluor staining

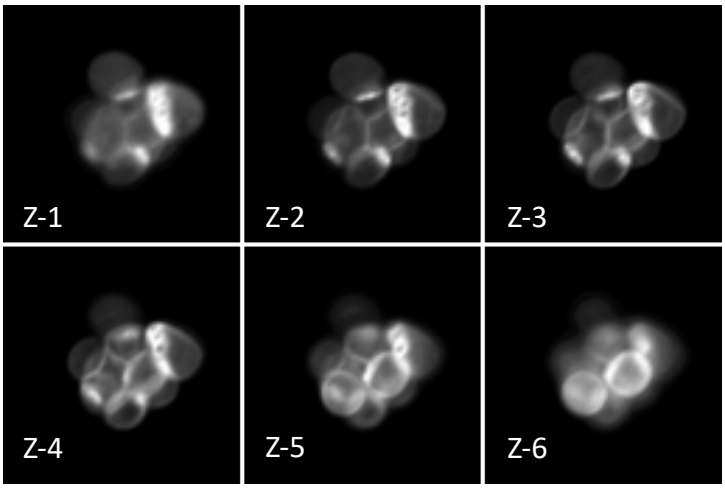

B

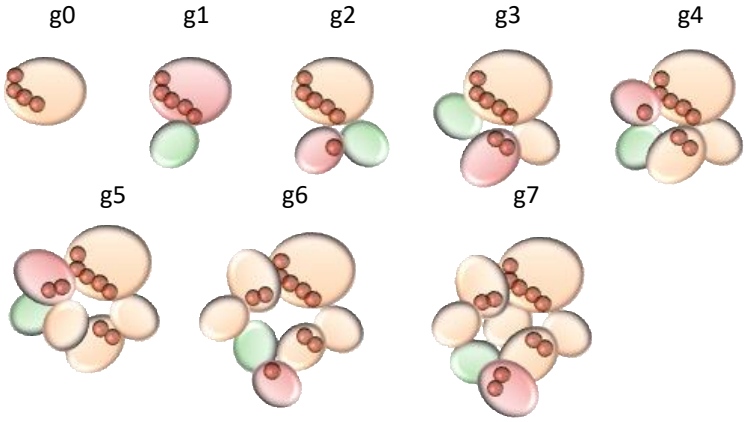

C

Calcofluor staining

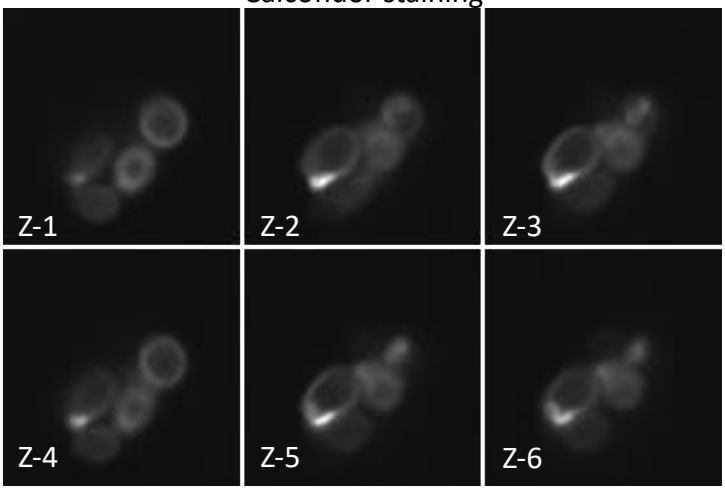

D

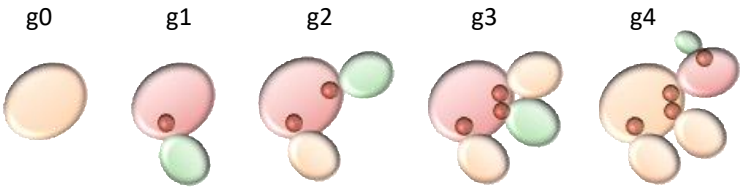

Figure 1. The proliferation pattern of slow-growing microcolonies can be isotropic or anisotropic. (A) Confocal images (Z stacks Z1-6) of a small microcolony taken after 13 hours of growth, stained with calcofluor in order to facilitate bud scar counting. This microcolony was founded by a non-newborn cell at generation 0 (g0). (**B**) Graphical representation of the development of the microcolony shown in (A) across generations (g1-g7). Every generation represents a cell division event. The new daughter cell generated in the last mitotic event is depicted in green, and the corresponding mother cell in red. Bus scars are represented in brown. In this case, no restriction for division was detected among the cells of the microcolony. We called *isotropic* to this non-restricted proliferation pattern. (**C**) Confocal images of another small microcolony, taken after 13 hours of growth and stained with calcofluor. This microcolony was founded by a newborn cell (g0). (**D**) Graphical representation of the development of the microcolony shown in (C) across generations (g1-g4). Doughter cells generated in g2 and g3 did not divide further, indicating a proliferation restriction in this microcolony. This restricted proliferation pattern was called *anisotropic*.

A

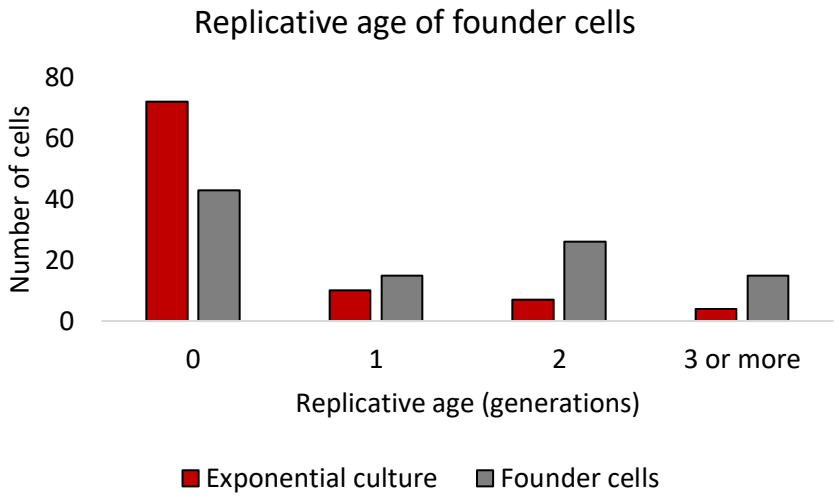
Replicative age of founder cells
Number of cells
80
60
40
20
0
0
1
2
3 or more
Replicative age (generations)
Exponential culture
Founder cells

B

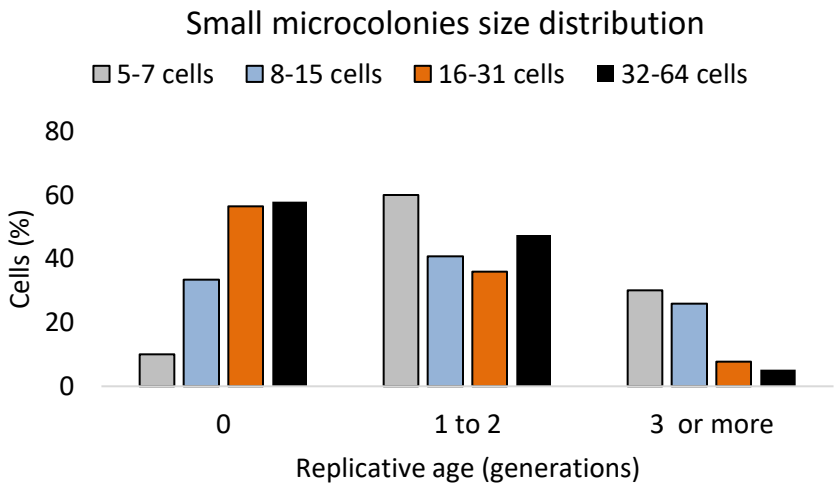
Small microcolonies size distribution
5-7 cells
8-15 cells
16-31 cells
32-64 cells
Cells (%)
80
60
40
20
0
0
1 to 2
3 or more
Replicative age (generations)

C

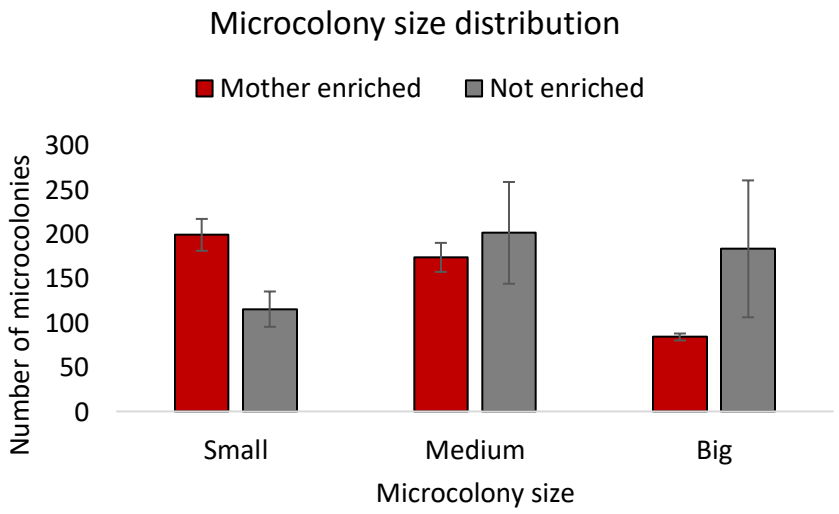
Microcolony size distribution
Mother enriched
Not enriched
Number of microcolonies
300
250
200
150
100
50
0
Small
Medium
Big
Microcolony size

Figure 2. Small microcolonies are more frequently founded by young mother cells than by newborns. **(A)** Distribution of founder cells (grey) according to their replicative age when founding the microcolony (n=96) compared to that of the initial exponential culture before encapsulation (red) (n=96). The two distributions exhibited significant statistical difference, according to a chi square test (p = 3,6 x 10^{-6}). (**B)** Comparison of the distributions of the replicative age of the founder cells (when founding) among small microcolonies of different size. We classified small microcolonies (those with less than 65 cells after 13 h of growth) into 4 categories, according to their number of cells: 32-64, 16-31, 8-15 and 5-7. The smaller the microcolony, the higher the proportion of non-newborn founder cells. A progressively increase in the proportion of microcolonies founded by mother cells with higher number of replication cycles can be observed in smaller categories. **(C)** Encapsulation of a population of cells enriched in young mothers with 1 or 2 division cycles, following the Mother Enrichment Program (see supplementary Figure S4A-B), produced a higher proportion of small microcolonies. Distribution of microcolonies according to their size (small, medium or big; see supplementary Figure S1A-B) from a control population (non-treated, in grey) and from a mother-enriched one (3 hours treatment, in red). Cultures enriched in young mothers produced a higher proportion of small microcolonies than a non-treated control. It is remarkable that more than 60% of the cells in this mother-enriched culture had a replicative age between 1 and 5, which means they were not old cells but young mothers. The two distributions exhibited significant statistical difference, according to a chi square test ($p < 10^{-6}$).

A

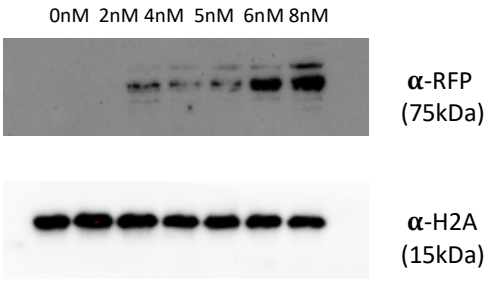
0nM 2nM 4nM 5nM 6nM 8nM
α-RFP
(75kDa)
α-H2A
(15kDa)

B

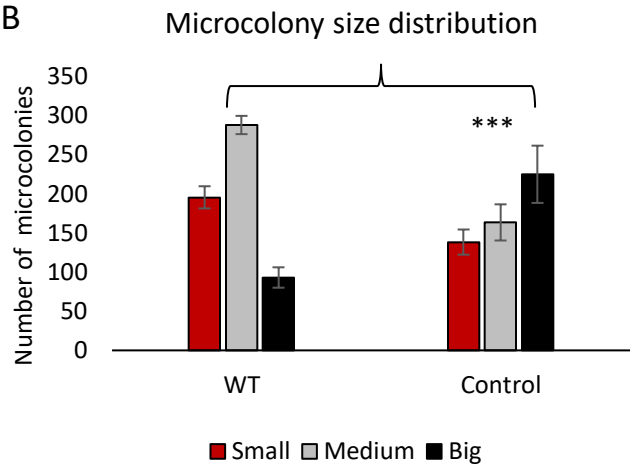
Microcolony size distribution
Number of microcolonies
350
300
250
200
150
100
50
0
***
WT
Control
Small
Medium
Big

C

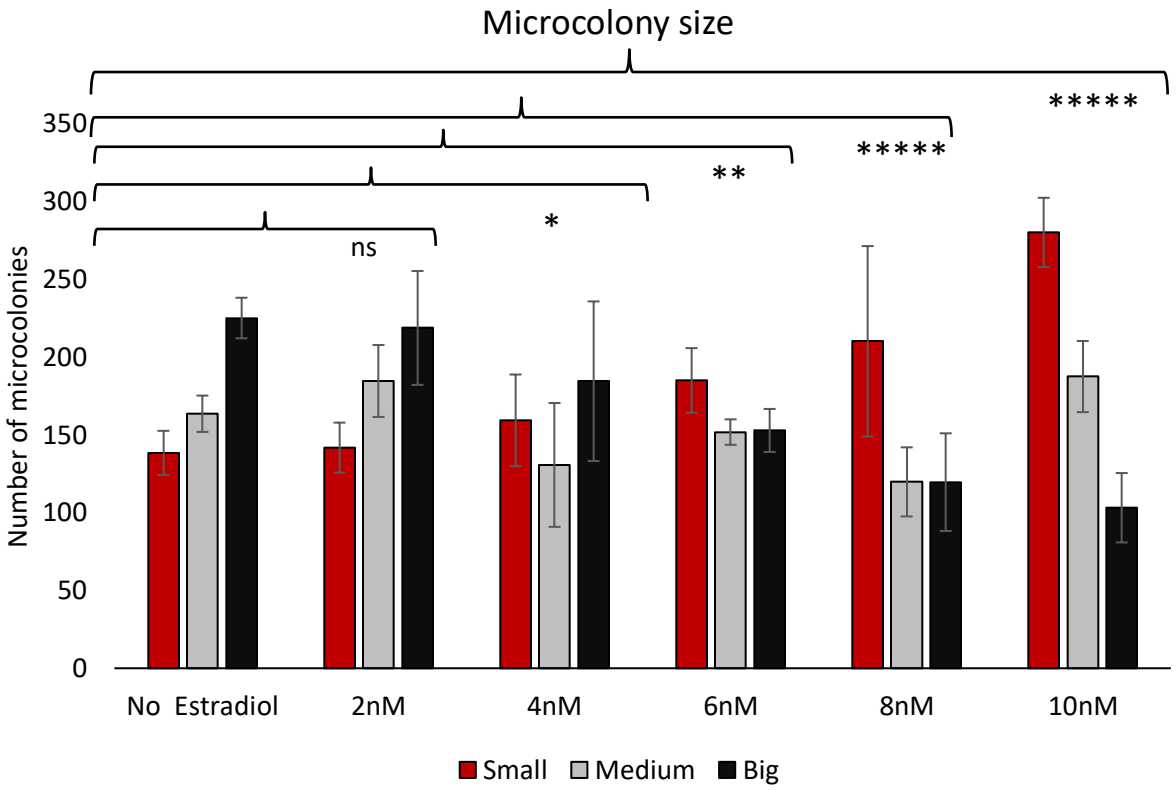
Microcolony size
Number of microcolonies
350
300
250
200
150
100
50
0
*****
*****
**
*
ns
No Estradiol
2nM
4nM
6nM
8nM
10nM
Small
Medium
Big

Figure 3. Upregulation of Whi5 levels provokes higher frequency of slow-proliferating microcolonies. (A) Western blot of inducible Whi5 strain KSY098 at different estradiol concentration. Whi5 accumulated in a dose-dependent manner according to the increasing concentration of estradiol in the media. **(B)** Comparison of the size distributions of microcolonies formed by KSY098 cells grown without estradiol and a WT control. Compared to the wildtype profile, lack of Whi5 expression produced a significantly different pattern, characterized by an increase in big microcolonies (black) and a decrease in small microcolonies (red). **(C)** Microcolony size distribution profile of KSY098 strain cultured without estradiol (control), or with 2, 4, 5, 6, 8 or 10nM, respectively. As estradiol concentration increases, and expression levels of Whi5 get proportionally higher, a progressive raise in the proportion of small microcolonies was detected. Square chi tests were performed for statistical significance. *, **, *** and ***** mean *p* values lower than 5×10^{-2}, 5×10^{-3}, 5×10^{-4} and 5×10^{-6} respectively.

A

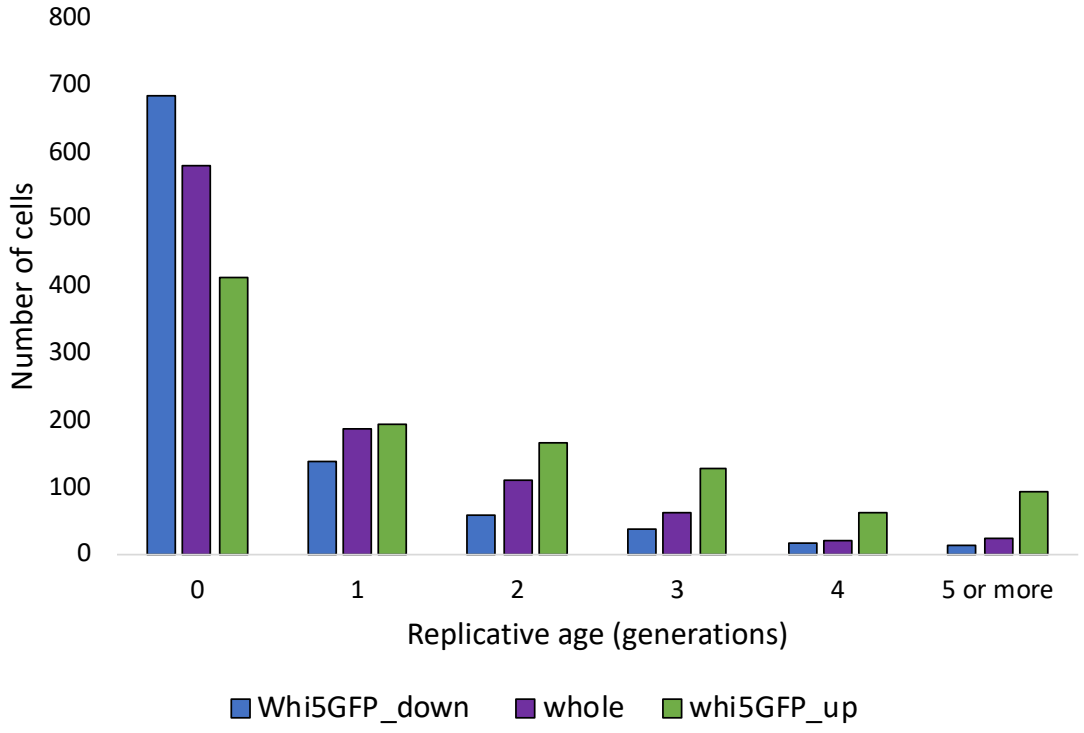
800
700
600
500
400
300
200
100
0
Number of cells
0
1
2
3
4
5 or more
Replicative age (generations)
Whi5GFP_down
whole
whi5GFP_up

B

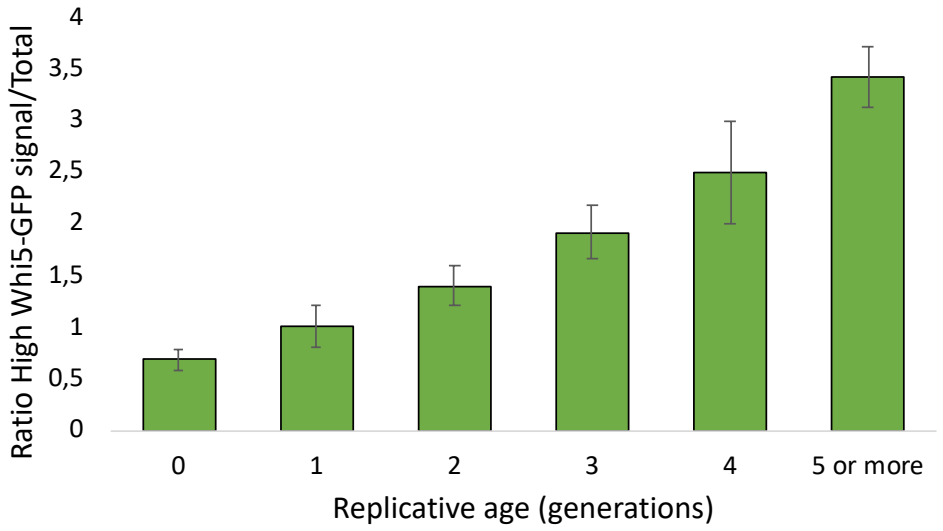
4
3,5
3
2,5
2
1,5
1
0,5
0
Ratio High Whi5-GFP signal/Total
0
1
2
3
4
5 or more
Replicative age (generations)

Figure 4. The proportion of cells expressing high Whi5 levels in young mothers is higher than in newborn cells. (A) Replicative age distribution, represented as the number of bud scars, for the whole population of cells (blue) and for Whi5 low-expressing (purple) and high-expressing (green) subpopulations. Bus scars were counted in three independent replicates of the experiment. In total, approximatively 1000 cells of each category were counted. The subpopulation of cells expressing higher levels of Whi5-GFP was enriched in young mothers with two or more division cycles, compared to the subpopulation with lower levels of Whi5-GFP, which was enriched in newborns. The difference between these two categories in terms of replicative age was statistically significant, according to a Chi square test (p = 0.02). **(B)** Ratio of cells with high Whi5 expression, relative to the whole population, in each replicative age group. For each biological replicate, the proportion of cells with a certain age in the High Whi5-GFP sample was divided by the corresponding proportion in the Whole population one. Average and standard deviations are shown. Frequency of high Whi5 expression increases with the number of mitotic cycles undergone, since the very first division. Statistical significance of the overall differences was confirmed with an ANOVA test ($p = 2.6 \times 10^{-5}$).

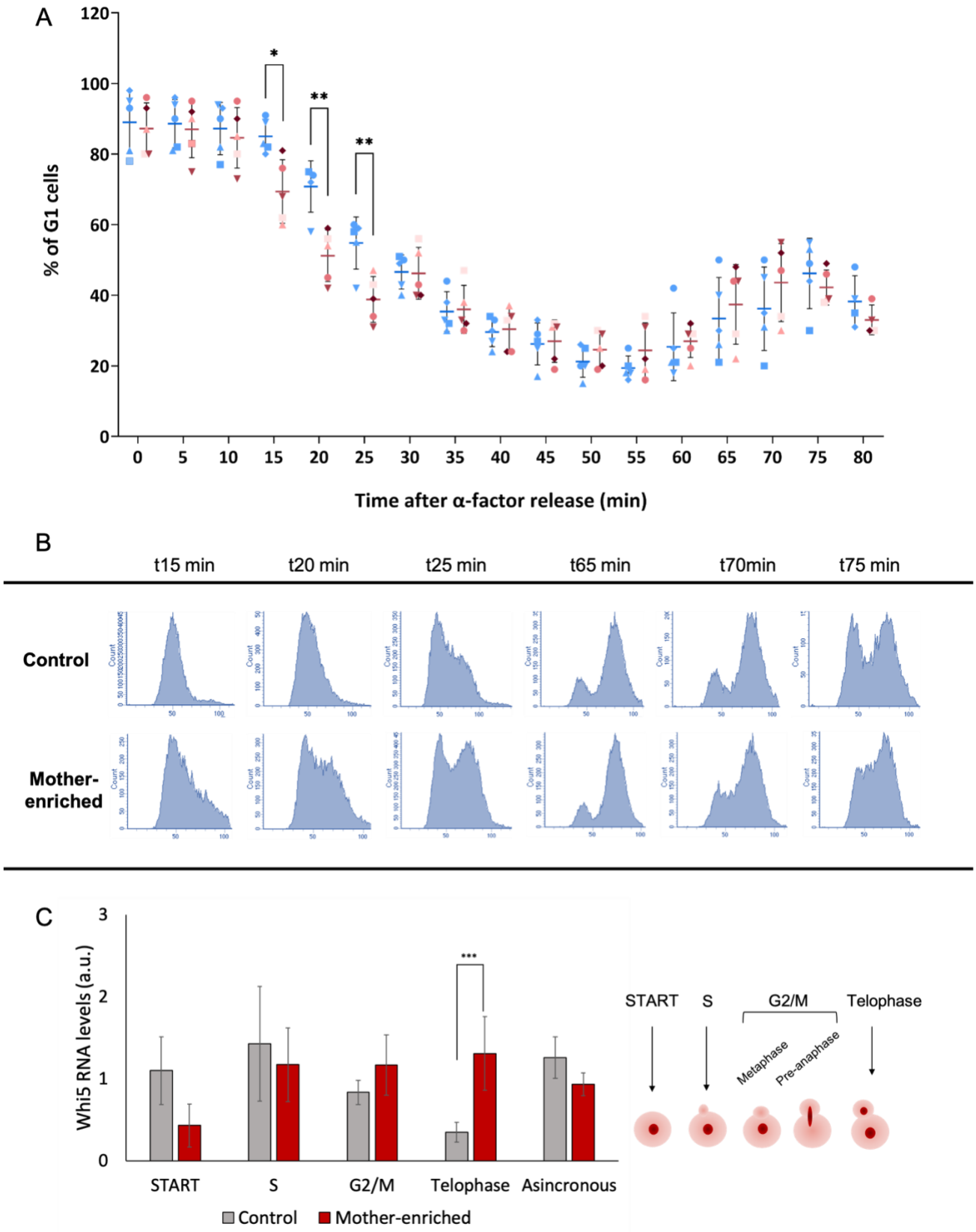
A
% of G1 cells
Time after α-factor release (min)
B
t15 min
t20 min
t25 min
t65 min
t70min
t75 min
Control
Mother-enriched
C
Whi5 RNA levels (a.u.)
START
S
G2/M
Telophase
Asincronous
Control
Mother-enriched
Metaphase
Pre-anaphase

Figure 5. Young mother cells spend longer time in S-G2-M than newborns and accumulate higher *WHI5* mRNA levels before cytokinesis. A) Cell-cycle progression through S-G2-M of cultures enriched in young mother cells with 3 to 5 divisions using the biotine/streptavidin method (see Materials an Methods) (pink), compared to control populations dominated by newborns (blue) (see supplementary Figure S7). Cells released from alpha-factor synchronization in START were sampled at the indicated times and analyzed by flow cytometry. Proportion of cells in G1 of 5 independent replicates are shown, each represented by a different symbol. For the first 10 minutes, both type of cultures remained synchronized in G1. However, at minute 15 mother-enriched cultures consistently entered S phase, while control cultures did not before minute 20. After minute 35, cells from both cultures progressed through G2-M in an almost identical manner until the next G1 pahse (after the 65 min time point). **B)** Flow cytometry of critical time points detected in A. **C)** Relative *WHI5* mRNA levels analyzed by RT-qPCR in mother-enriched (red) and control cultures (grey). Samples from 3 replicates of each type of culture, manipulated as in A, were taken at the times described in Table S2 and analyzed by flow cytometry and microscopy to be sure that they corresponded to the exact step of the cell cycle that was looked for. We observed that *WHI5* mRNA peaked in S phase in control cultures but stayed high until telophase in mother-enriched cultures.

Table 1. Growth patterns and founder cells of slow-proliferation microcolonies. Small microcolonies were classified as “isotropic” when most cells within that microcolony divided equally. They were classified as “anisotropic” when one cell (either the founder, or a first-born cell) underwent most divisions within the microcolony. In all cases, the founder cell was identified and classified into newborn or non-neborn (mother). Independently of the growth pattern, slow proliferation microcolonies tend to be founded by mother cells. See the text for details.

Type of slow growth	Number	Founder cell	Number
Isotropic	83	**Newborn**	39
		Mother	44
Anisotropic	10	**Newborn**	1
		Mother	9